JTTEE5 15:553-558
DOI: 10.1361/105996306X146884
1059-9630/$19.00 © ASM International

Peer Reviewed

Modeling of Motion and Heating of Powder Particles in Laser, Plasma, and Hybrid Spraying

Yu. Borisov, A. Bushma, and I. Krivtsun

(Submitted February 28, 2006; in revised form July 19, 2006)

Mathematical models for simulation of motion and heating of fine ceramic particles in plasma and laser spraying, as well as under conditions of a new technological process, that is, hybrid laser plasma spraying, are proposed. Trajectories, velocities, and temperature fields of fine SiO_2 particles being sprayed using the argon plasma jet, CO_2 laser beam, and their combination have been calculated. It is shown that the space-time distribution of temperature in spray particles greatly depends on the spraying method.

Keywords CO_2 laser, plasma jet, laser plasma spray process, numerical modeling, SiO_2 feedstock

1. Introduction

The processes of surface modification and deposition of coatings using laser radiation are now receiving an increasingly wide acceptance. One such process is laser spraying. The main point of this process is that powder particles are fed into the laser beam, heated, and melted by the laser radiation, accelerated with a gas flow and then deposited on the workpiece surface (Ref 1). This process can be implemented using laser radiation of different wavelengths (CO_2 or Nd:YAG lasers), various methods and systems for beam focusing, as well as methods for feeding powder to the heating zone (Ref 2, 3). In particular, CO_2 lasers are mostly demonstrated for laser spraying of coatings of ceramic materials (Al_2O_3, ZrO_2), as these materials absorb radiation with a wavelength of λ = 10.6 μm much better than the short-wave radiation (λ = 1.06 μm) of the Nd:YAG lasers (Ref 4).

The process under consideration has a number of advantages, compared with the well-known technologies of plasma spraying of ceramic coatings. First of all, it should be noted that CO_2 laser radiation is characterized by a high efficiency of heating of finely dispersed ceramic materials (Ref 5). In addition, unlike plasma heating, where the heat source in a particle is of the surface type, in the case of laser heating of dielectric particles, the size of which is commensurable with the radiation wavelength, absorption of the energy takes place within the entire volume of a particle (Ref 5, 6). This provides volume heating and complete melting of the spray particles, thus improving quality of a resulting coating.

The aforementioned peculiarities of laser heating of ceramic particles are of special interest for development and realization of the efficient process of deposition of SiO_2 coatings by thermal spraying. This material has a number of important service properties (mechanical, physical-chemical, electric), but due to a peculiar crystalline frame structure, this oxide is characterized by a delayed transition from the solid to fully molten state, and the viscosity of the cellular melt at the initial melting stage being very high, that is, 2.9×10^5 kg/(m · s) at 1993 K (Ref 7). This hampers deformation of the spray particles at their collision with the substrate and prevents formation of a coating layer (Ref 8).

Drawbacks of the laser spraying process include the fact that its practical realization requires high-power laser units, the price of which is very high but the efficiency is no more than 10%, which makes this process much more expensive than plasma spraying. In addition, in laser spraying with a coaxial feed of powder to the focused laser beam (Ref 2), the presence of a small size zone of a high radiation intensity (beam waist zone) makes it very difficult to ensure high process productivity and powder utilization.

One of the ways of addressing the aforementioned problems can be the use of a new technological process—hybrid laser plasma spraying. This process consists of combining the laser beam and plasma jet to exert a joint thermal effect on spray particles (this process should not be confused with the known method of laser treatment of coatings that were deposited first, for example, by plasma spraying, Ref 1). An important feature of the hybrid process implemented using the CO_2 laser is a direct interaction of laser radiation with the arc plasma, which may change the characteristics of both the plasma jet and the laser beam (Ref 9). In this case, their effect on the spray materials can be of a synergic character.

The combination offered makes it possible to combine advantages and overcome drawbacks of the existing spraying methods (laser and plasma) taken separately. In particular, an additional use of the plasma jet will allow a substantial decrease in laser power required for the spraying process to occur and will eventually raise the process productivity and material utilization.

On the other hand, a combination of the plasma (surface) and

This article was originally published in *Building on 100 Years of Success, Proceedings of the 2006 International Thermal Spray Conference* (Seattle, WA), May 15-18, 2006, B.R. Marple, M.M. Hyland, Y.-Ch. Lau, R.S. Lima, and J. Voyer, Ed., ASM International, Materials Park, OH, 2006.

Yu. Borisov, A. Bushma, and **I. Krivtsun,** E.O. Paton, Electric Welding Institute of NASU, Kiev, Ukraine. Contact e-mail: krivtsun@paton.kiev.ua.

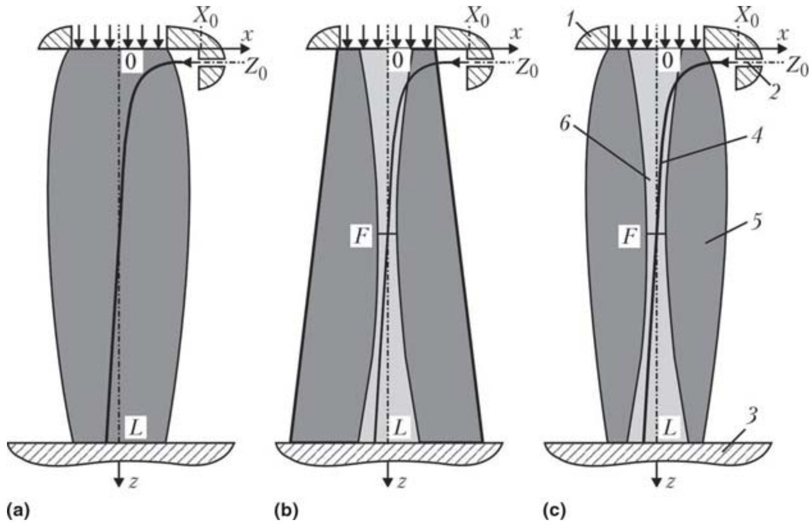

Fig. 1 Flow diagrams of (a) plasma, (b) laser, and (c) hybrid laser-plasma spraying processes. 1, plasma torch nozzle; 2, powder injector; 3, workpiece; 4, path of a spray particle; 5, plasma jet; 6, laser beam; 7, cold gas flow

laser (volume) methods for heating ceramic particles will provide complete melting of the particles when reaching the workpiece surface, which is required for the formation of high-quality coatings.

Figure 1 illustrates the plasma and laser spraying processes considered in this study, as well as the hybrid process implemented by coaxial joining of the plasma jet and laser beam using an integrated (laser + nontransferred arc) plasma torch (Ref 9). In the first case (Fig. 1a), the spray particles are accelerated and heated with the plasma jet, and in the second case (Fig. 1b), they are accelerated with a cold gas flow and heated by laser radiation. In the third case (Fig. 1c), the particles are accelerated with the plasma flow and heated both by the plasma jet and the laser radiation.

The most important indicators of all these processes are characteristics of the motion and heating of the spray particles. As experimental investigation of these characteristics can be difficult, it is therefore the purpose of this study to provide theoretical description and mathematical modeling of the motion and heating of ceramic particles when using different spraying methods.

2. Model of Particle Motion

The velocity and trajectory of a spray particle can be calculated using equations of motion:

$$m\frac{d\mathbf{v}}{dt} = \mathbf{F} \qquad \text{(Eq 1)}$$

Here m is the mass of a particle, $\mathbf{v}(t) = (v_x, v_y, v_z)$ is the current value of the velocity vector of the particle at time t in the coordinate system shown in Fig. 1 with the y-axis pointing out of the paper, and $\mathbf{F}$ is the force acting on the particle located in the flow of plasma or the cold gas. Equation 1 can be integrated under the initial conditions:

$$\begin{aligned} &x|_{t=0} = X_0 \quad &&y|_{t=0} = 0 \quad &&z|_{t=0} = z_0 \\ &v_x|_{t=0} = -v_0 \quad &&v_y|_{t=0} = 0 \quad &&v_z|_{t=0} = 0 \end{aligned} \qquad \text{(Eq 2)}$$

where X_0 and Z_0 are the coordinates of the point at which the particle leaves the powder injector (Fig. 1), and v_0 is the initial velocity the particle acquires in the carrier gas flow.

To analyze the motion of a spray particle, the particle is considered to be spherical and having radius a, and it is assumed that the particle in the plasma jet (a cold gas flow) is affected only by the viscous drag force (Ref 10):

$$\mathbf{F} = C_d S \frac{\rho_p(\mathbf{u}-\mathbf{v})|\mathbf{u}-\mathbf{v}|}{2} \qquad \text{(Eq 3)}$$

Here C_d is the viscous drag coefficient, $S = \pi a^2$ is the cross-sectional area of the particle, and ρ_p and $\mathbf{u}$ are the density and velocity of the undisturbed flow of plasma or cold gas at the location of the particle. To determine the particle aerodynamic drag coefficient, the criterial dependencies are used (Ref 11):

$$\begin{aligned} &C_d = 24\,Re^{-1} \text{ at } Re < 0.2 \\ &C_d = 24\,Re^{-1} + 3.6\,Re^{-0.317} \text{ at } 0.2 < \mathrm{Re} < 4 \\ &C_d = 24\,Re^{-1} + 4\,Re^{-0.333} \text{ at } 4 < \mathrm{Re} < 400 \end{aligned} \qquad \text{(Eq 4)}$$

where $Re = (\rho_p|\mathbf{u}-\mathbf{v}|2a)/\mu_p$ is the Reynolds number, and μ_p is the coefficient of dynamic viscosity of undisturbed plasma or gas flow at the location of the particle. To take into account the variations of plasma properties within the thermal boundary layer near the particle one can use factor $(\rho_p\mu_p/\rho_s\mu_s)^{-0.45}$ as the correction coefficient for C_d (Ref 10) (index s designates the corresponding properties of plasma at a temperature on the particle surface).

3. Model of Particle Heating

The temperature field of a spherical particle heated by the laser beam, plasma jet, or their combination is calculated in general using the nonstationary heat conduction equation with a distributed heat source. Assuming a spherical symmetry of the temperature field of the particle, and allowing for the temperature dependence of properties of its material, this equation can be written in the form:

$$\rho\overline{C}\frac{\partial T}{\partial t}=\frac{1}{r^2}\frac{\partial}{\partial r}\left(r^2\chi\frac{\partial T}{\partial r}\right)+D \quad \text{(Eq 5)}$$

Here $T(r, t)$ is the space-time distribution of temperature in the particle (r is the distance from the particle center and t is the time), $\rho(T)$ is the density, $\chi(T)$ is the thermal conductivity, and $\overline{C}(T)$ is the effective heat capacity of the particle material calculated with allowance for latent melting heat W_M and vapor formation W_B:

$$\overline{C}=c+W_M\delta(T-T_M)+W_B\delta(T-T_B) \quad \text{(Eq 6)}$$

where $c(T)$ is the specific heat of the material, T_M and T_B are the melting and boiling temperatures, respectively, and $\delta(x)$ is the delta function.

In the case of laser and combined heating, the $D(r, t)$ value of Eq 5 describing the energy source in the bulk of a particle due to absorption of laser radiation is determined by (Ref 5):

$$D=\frac{S^{\rm inc}\varepsilon_l''}{8k}\sum_{m=1}^{\infty}(2m+1)\sum_{\gamma=1,2}\{|d_\gamma^{(l)}|^2F_\gamma^{(l)}+2Re[d_\gamma^{(l)}\tilde{d}_\gamma^{(l)*}H_\gamma^{(l)}] + |\tilde{d}_\gamma^{(l)}|^2G_\gamma^{(l)}\} \quad \text{(Eq 7)}$$

Here $S^{\rm inc}$ is the local value of the intensity of laser radiation at the location of the particle, $k = 2\pi/\lambda$ is its wave vector, ε'' is the imaginary part of the complex dielectric permittivity of the particle material, while functions $F_{1,2}^{(l)}(r)$, $H_{1,2}^{(l)}(r)$, $G_{1,2}^{(l)}(r)$, as well as values $d_{1,2}^{(l)}$, $\tilde{d}_{1,2}^{(l)}$ are determined in Ref 5. In modeling of plasma heating of the particle, the volume heat source in the heat conduction equation is assumed to be zero.

Initial and boundary conditions for Eq 5 can be written as:

$$T(r)|_{t=0}=T^0$$
$$\left(\chi\frac{\partial T}{\partial r}\right)\bigg|_{r=a}=q \qquad \frac{\partial T}{\partial r}\bigg|_{r=0}=0 \quad \text{(Eq 8)}$$

where T^0 is the initial temperature of the particle, and $q(t)$ is the current value of a heat flux through its surface. In the case of plasma and combined heating, this value can be calculated from the formula (Ref 12):

$$q=h(T_p-T_s)+\xi\sigma_0(T_p^4-T_s^4) \quad \text{(Eq 9)}$$

Here T_p is the temperature of undisturbed plasma flow at the particle location point, $T_s(t)$ is the current value of the particle surface temperature, h is the heat exchange coefficient, ξ is the reduced emissivity factor for the plasma-particle surface system, and σ_0 is the Stefan-Boltzmann constant.

The coefficient of convective heat exchange for a spherical particle can be calculated based on the criterial dependence for a flow about a sphere (Ref 11):

$$Nu=2\frac{\chi_s}{\chi_p}+0.5\,Re^{0.5}\,Pr^{0.4}\left(\frac{\rho_p\mu_p}{\rho_s\mu_s}\right)^{0.2} \quad \text{(Eq 10)}$$

where $Nu = (\alpha 2a)/\chi_p$ is the Nusselt number, $Pr = (C_p\mu_p)/\chi_p$ is the Prandtl number, and χ_p and C_p are the thermal conductivity coefficient and specific heat of undisturbed plasma flow at the particle location point (index s designates the corresponding properties of plasma at a temperature on the particle surface). In the simulation of laser heating, it is assumed that a particle being heated moves in a jet of cold gas at temperature T^0. In this case, the heat flux from its surface can also be described by relationships Eq 9 and 10 by assuming $T_p = T^0$.

To close the above models describing the processes of motion and heating of spray particles, it is necessary to determine the spatial distributions of temperature and velocity of the plasma jet (in the case of plasma and hybrid spraying), the velocity of a cold gas flow (in the case of laser spraying), and the intensity of the laser radiation (in the case of laser and hybrid spraying). Calculation of the distribution of temperature T_p and velocity **u** of plasma in a jet generated by the nontransferred arc plasma torch was made using the CASPSP software (Ref 13). This computer model of the plasma jet is based on a mathematical model of gas dynamics and heat transfer for the turbulent flow of the arc plasma, described by a system of magnetic-gas-dynamic (MGD) equations.

The spatial distribution of the velocity of a cold gas flow is determined from a condition that the gas jet is emitted from a cylindrical nozzle with diameter d into a quiescent environment (submerged turbulent jet). Distribution of an axial component of the gas velocity in such a jet can be set in the form (Ref 14):

$$u_z=u_0\exp\left[-4.33\frac{(x^2+y^2)}{r_j^2}\right] \quad \text{(Eq 11)}$$

Here $u_0 = 4.19\,G\,z/r_j^2\,d$ is the axial gas velocity at the jet axis, G is the volume gas flow rate, $r_j(z) = d/2 + z\text{tg}\beta$ is the current radius of the jet, and $\beta = 12.5°$ is its divergence angle (Ref 14). When determining the spatial distribution of the radiation intensity in the laser beam, it is assumed that the beam is Gaussian (TEM_{00} mode), having a minimal transverse size in plane $z = F$ (Fig. 1). In this case, the $S^{\rm inc}$ value can be determined from the relationship:

$$S^{\rm inc}=S^0\exp\left[-\frac{2(x^2+y^2)}{r_b^2}\right] \quad \text{(Eq 12)}$$

where $S^0 = 2Q^0/\pi r_b^2$ is the intensity of radiation at the beam axis, Q^0 is the total power of the laser beam, and $r_b(z)$ is its radius:

$$r_b^2=r_F^2\left[1+\frac{(z-F)^2}{z_F^2}\right] \quad \text{(Eq 13)}$$

where r_F is the radius of the beam in a focal plane, and $z_F = kr_F^2/2$ (Ref 15).

4. Simulation of Particle Motion and Heating

Numerical analysis of the motion and heating of particles under conditions of plasma, laser, and hybrid spraying was conducted using the approximation of a low-dusted jet; that is, it was assumed that loading of the jet with a powder was low and hardly affected the distribution of the thermal and dynamic character-

Peer Reviewed

istics of the flow. It was also assumed that the spray particles had a small effect on the characteristics of the laser beam (approximation of weak absorption). Furthermore, it is assumed in this study that under the hybrid process conditions, no allowance was made for the direct interaction of the focused laser radiation with the plasma jet; that is, the spatial distributions of their characteristics were assumed to be the same as in the case of independent heat sources. The latter approximation is well justifiable, unless the temperature of the plasma jet at the laser beam axis is higher than 11×10^3 K (for the atmospheric pressure argon plasma) (Ref 9).

Figure 2 shows the calculation results of the trajectory and axial velocity of a SiO_2 particle of 30 μm radius, moving in an argon plasma jet generated by a plasma torch with a smooth anode nozzle of 5 mm in diameter and 8 mm long, arc current I = 200 A and plasma gas flow rate G = 30 L/min (arc voltage 30.9 V, plasma torch efficiency 67%). Figure 2 also shows the corresponding results for a particle moving in a jet of cold gas (argon at temperature T^0 = 300 K) emitted from the nozzle with diameter d = 6 mm at G = 70 L/min. Coordinates of the point of exit of the particle from the powder injector in both cases were identical: $X_0 = Z_0$ = 5 mm, initial velocity of the particle was v_0 = 7.4 m/s at the entrance to the plasma jet and v_0 = 3.6 m/s at entrance to the cold gas flow (the values of v_0 were selected so that particles intersected the jet axis at distance $z = F$ = 6 cm from the exit section of the nozzle and had close values of the axial velocity in reaching the substrate). It should be noted that, as the effect of laser radiation on the thermal and dynamic characteristics of the plasma jet are ignored, in a case of the hybrid process the calculated path and velocity of a particle will be the same as in the case of plasma spraying. As to the approximations of the low-dusted jet and weak absorption of the laser beam used at the selected values of the particle radius and gas flow rate under consideration, these approximations are well justifiable at a powder feed rate of not more than 1 kg/h (volume fraction of dispersed phase κ is about 1×10^{-4}, which is lower than $\kappa_{cr} = 4 \times 10^{-4}$ for the low-dusted flows, Ref 16).

Figure 3 shows the time variations along the z-axis in the calculated values of the temperature at the center, T_c, and on the surface, T_s, of the SiO_2 particle in the plasma, laser, and hybrid

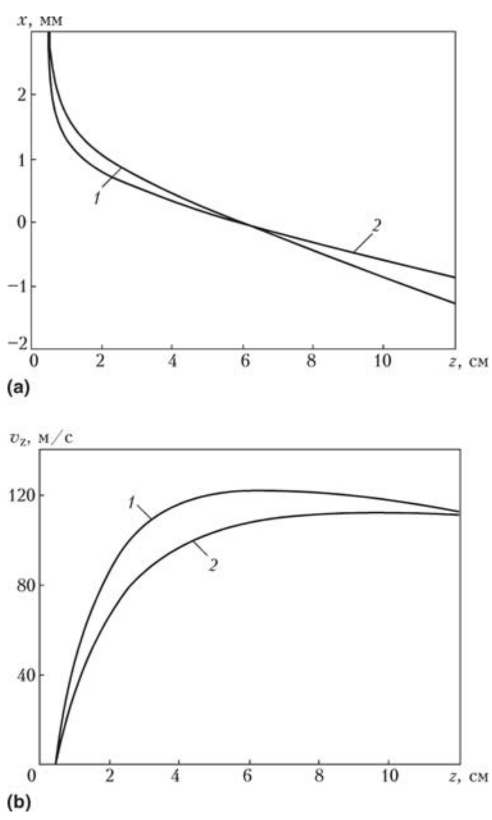

Fig. 2 (a) Trajectories and (b) velocities of SiO_2 particles 60 μm in diameter in a jet of argon plasma (curve 1) and flow of cold gas (curve 2) along the z-axis

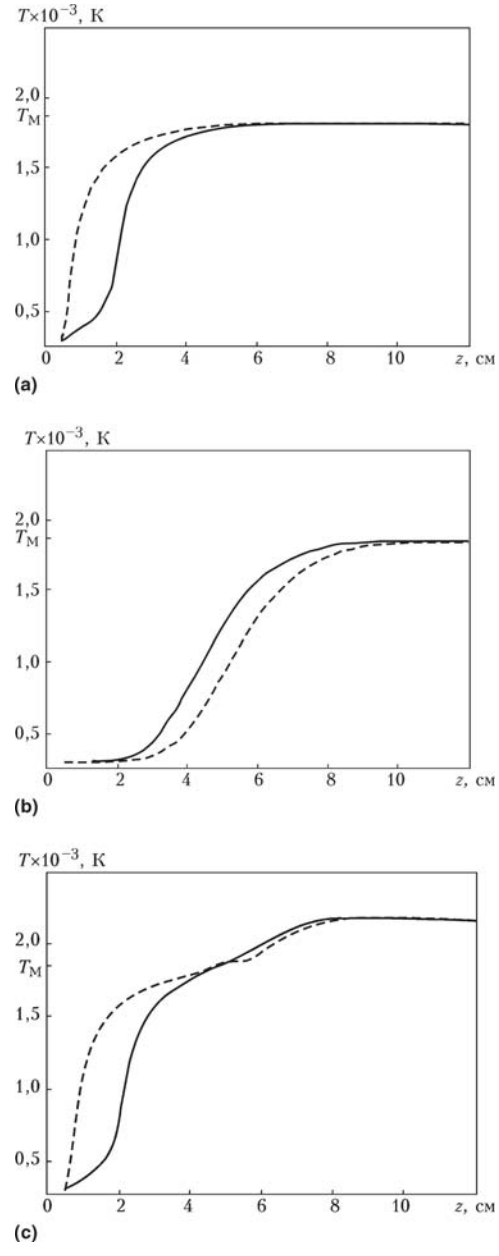

Fig. 3 Temperature at the center (solid curves) and on the surface (dashed curves) of SiO_2 particle 60 μm in diameter heated by the (a) argon plasma jet, (b) 0.5 kW CO_2 laser beam, and (c) their combination along the z-axis

spraying. Parameters of the plasma jet and the cold gas jet were selected as noted previously, while parameters of the laser beam were: $Q^0 = 0.5$ kW, $r_F = 0.25$ mm and $F = 6$ cm.

As proved by the calculation data shown in Fig. 3(a), the values of T_s in plasma (surface) heating of the considered particle are higher than the values of T_c, whereas in the case of laser heating the situation is reversed (Fig. 3b), which is caused by the volume character of heat generated in the particle (Ref 5, 6).

In addition, heating of a particle occurs slower and begins later (comparing Fig. 3a and b). This is associated with the fact that, due to the small transverse sizes of the laser beam, the particle gets to the heating zone later than in plasma spraying. It should be noted at this point that in both cases (with the selected values of the plasma and laser beam parameters) the particle temperature does not reach the melting temperature of SiO_2.

As far as hybrid spraying is concerned, the particle heating process can be conditionally subdivided into two stages (Fig. 3c). At the first stage, when getting into the plasma jet, the particle is preliminarily heated by the plasma ($T_s > T_c$). Then, getting into the laser beam, it experiences an extra laser heating, so that T_c becomes a bit higher than T_s. Finally, when reaching the substrate, the particle is uniformly heated and fully melted as the particle temperature exceeds the melting temperature of SiO_2.

Similar results can be achieved in the case of laser spraying of particles, but using the laser beam with power twice as high (comparing Fig. 3c, and Fig. 4a). Therefore, using additional plasma jet allows the power of the laser radiation required for the spraying process to be substantially decreased.

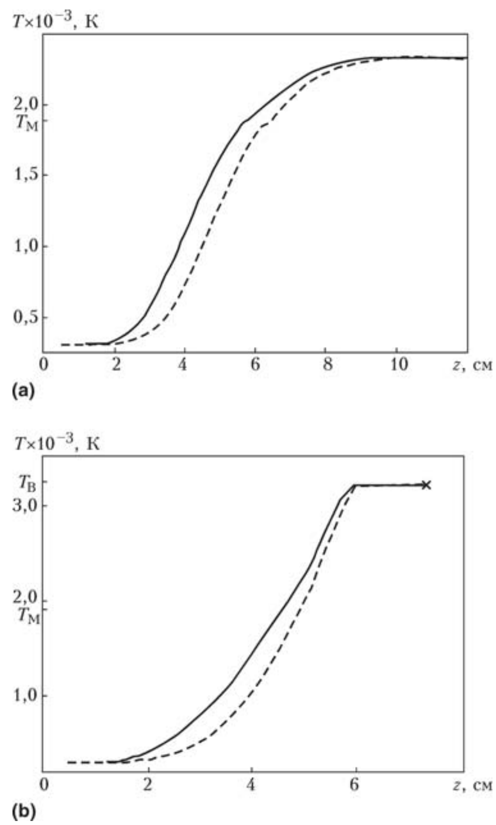

Fig. 4 Temperature at the center (solid curves) and on the surface (dashed curves) of SiO_2 particle 60 μm in diameter heated by the (a) 1.0 and (b) 2.5 kW CO_2 laser beam along the z-axis; × denotes thermal explosion of the particle

An interesting peculiarity of the process of laser heating of fine ceramic particles in the case of using higher-power laser beams is the earlier noted effect of thermal explosion of the particles (Ref 5). Thus, getting to the area of high values of the radiation intensity, a SiO_2 particle with a diameter of 60 μm is heated to temperatures close to the boiling point of the material (Fig. 4b).

Besides, due to a more intensive heating of the central regions of the particle (Ref 5, 6), the evaporation conditions are realized at the distance 4.5 μm from the particle center; that is, thermal explosion of the particle takes place. This allows splitting of particles near the workpiece surface by properly selecting the power and conditions of focusing of the laser beam, as well as conditions of introduction of powder into the heating zone, which may have a positive effect on the quality of the resulting coating.

5. Summary and Conclusions

In general, the results of numerical modeling of the characteristics of heating of powder particles in plasma, laser, and hybrid spraying of coatings are indicative of a promising future of development and practical application of the latter method. These results can also be used for the design of specialized equipment (e.g., integrated laser arc plasma torches) and elaboration of technological principles for hybrid laser plasma spraying.

References

1. L. Pawlowski, Thick Laser Coatings: A Review, *J. Therm. Spray Technol.,* 1999, **8**(2), p 279-295
2. T.R. Tucker, A.H. Clauser, I.G. Wright, and J.T. Stropki, Laser-Processed Composite Metal Cladding for Slurry Erosion Resistance, *Thin Solid Films,* 1984, **118,** p 73-84
3. H. Kindler, R. Volz, and M. Huonker, Ein Neues Verfarhren zum Laserbeschichten, *The Sixth European Conference on Laser Treatment of Materials* (Stuttgart, Germany), Sept 16-19, 1996, F. Dausinger, Ed., AWT, Wiesbaden, Vol. 1, 1996, p 447-454, in German
4. V.M. Zolotarev, V.N. Morozov, and E.V. Smirnova, *Optical Constants of Natural and Technical Media: Manual,* Khimiya, Leningrad, 1984, in Russian
5. A.I. Bushma and I.V. Krivtsun, Peculiarities of Laser Radiation Heating of Fine Ceramic Particles, *Fiz. Khim. Obrab. Mater.,* 1992, (2), p 40-48, in Russian
6. A.I. Bushma and I.V. Krivtsun, Peculiarities of Absorption and Scattering of Different Wavelength Laser Radiation by Fine Spherical Particles, *Int. Conf. on Laser Technologies in Welding and Materials Processing* (Katsiveli, Crimea, Ukraine), May 19-23, 2003, B.E. Paton and V.S. Kovalenko, Ed., E.O. Paton Electric Welding Institute, NASU, 2003, p 103-107
7. A.R. Ubbelode, *Molten State of Matter,* Metallurgiya, Moscow, 1982, in Russian
8. Yu.S. Borisov, Yu.A. Kharlamov, S.L. Sidorenko, and E.N. Ardatovskaya, *Thermal Spray Coatings of Powder Materials,* Naukova Dumka, Kiev, Ukraine, 1987, in Russian
9. P. Seyffarth and I.V. Krivtsun, *Laser-Arc Processes and their Applications in Welding and Materials Treatment,* Taylor and Francis Books, London, UK, 2002
10. E. Pfender and Y.C. Lee, Particle Dynamics and Particle Heat and Mass

Transfer in Thermal Plasmas. Part I. The Motion of a Single Particle without Thermal Effects, *Plasma Chem. Plasma Process.,* 1985, **5**(3), p 211-237

11. Yu.V. Tsvetkov and S.A. Panfilov, *Low-Temperature Plasma in Repair Processes,* Nauka, Moscow, 1980, in Russian
12. Y.C. Lee, Y.P. Chyou, and E. Pfender, Particle Dynamics and Particle Heat and Mass Transfer in Thermal Plasmas. Part II. Particle Heat and Mass Transfer in Thermal Plasmas Effects, *Plasma Chem. Plasma Process.,* 1985, **5**(4), p 391-414
13. Yu. Borisov, I. Krivtsun, and A. Muzhichenko, Computer Modelling of the Plasma Spraying Process, *Thermal Spray 2003: Advancing the Science & Applying the Technology,* B. Marple and C. Moreau, Ed., ASM International, 2003, p 1001-1009
14. L.D. Landau and E.M. Lifshits, *Hydrodynamics,* Nauka, Moscow, 1986, in Russian
15. A. Yariv, *Quantum Electronics,* John Wiley & Sons, New York, 1975
16. Z.R. Gorbis, *Heat Exchange and Hydrodynamics of Dispersed Through Flows,* Energiya, Moscow, 1970, in Russian